

Supplementary Information

Removal of bisphenol A by iron nanoparticles doped magnetic ordered mesoporous carbon

Lin Tang^{, a,b}, ZhihongXie^{a,b}, GuangmingZeng^{*,a,b}, Haoran Dong^{a,b}, Changzheng Fan^{a,b}, Yaoyu*

Zhou^{a,b}, Jiajia Wang^{a,b}, Yaocheng Deng^{a,b}, Jingjing Wang^{a,b}, Xue Wei^{a,b}

^aCollege of Environmental Science and Engineering, Hunan University, Changsha, 410082, China,

^bKey Laboratory of Environmental Biology and Pollution Control (Hunan University), Ministry of Education, Changsha 410082, Hunan, PR China.

*Corresponding author: Tel.: +86-731-88822778; Fax.: +86-731-88823701

E-mail: tanglin@hnu.edu.cn (L. Tang) , zgming@hnu.edu.cn (G.M. Zeng)

Total number of pages of Supporting Information: 11

Number of Figures in Supporting Information: 8

Number of Tables in Supporting Information: 2

List of Supplemental Figures

Fig. S1 Nitrogen adsorption–desorption isotherms. Inset: pore size distribution of OMC and Fe/OMC.

Fig. S2 Zeta potentials of Fe/OMC. Inset: the magnetization curves of Fe/OMC.

Fig. S3 Thermogravimetric analysis curves of Fe/OMC.

Fig. S4 Effect of pH values on removal of BPA by Fe/OMC at 25 °C, within 6h (initial concentration, 200 mg/L).

Fig. S5 Effect of contact time and initial concentration on removal of BPA by Fe/OMC at 25 °C.

Fig. S6 Pseudo-second-order kinetic model for the adsorption of BPA onto Fe/OMC at 25 °C

Fig. S7 Adsorption isotherms for adsorption of BPA onto Fe/OMC.

Fig. S8 Six consecutive adsorption–desorption cycles of Fe/OMC

Table S1 Pore structure parameters of the two mesoporous materials.

Table S2 The chemical characterization results obtained by each analytical technique.

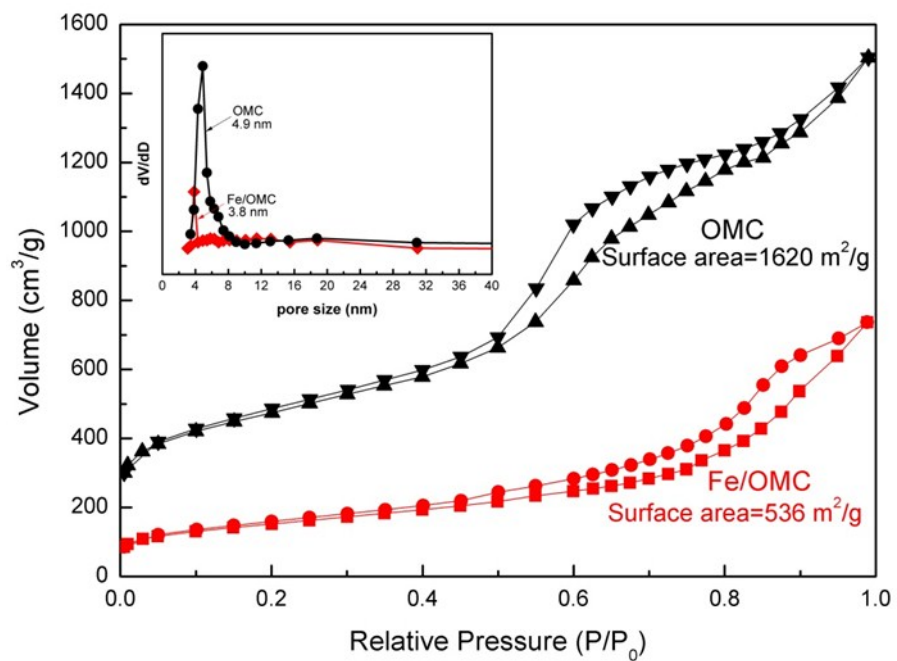


Fig. S1 Nitrogen adsorption-desorption isotherms. Inset: pore size distribution of OMC and Fe/OMC

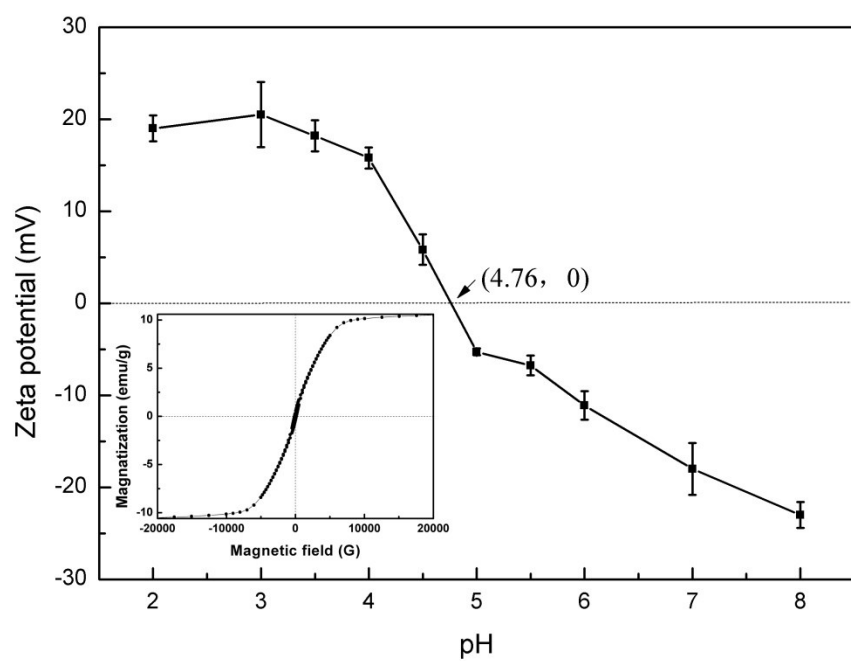


Fig. S2 Zeta potentials of Fe/OMC. Inset: the magnetization curves of Fe/OMC

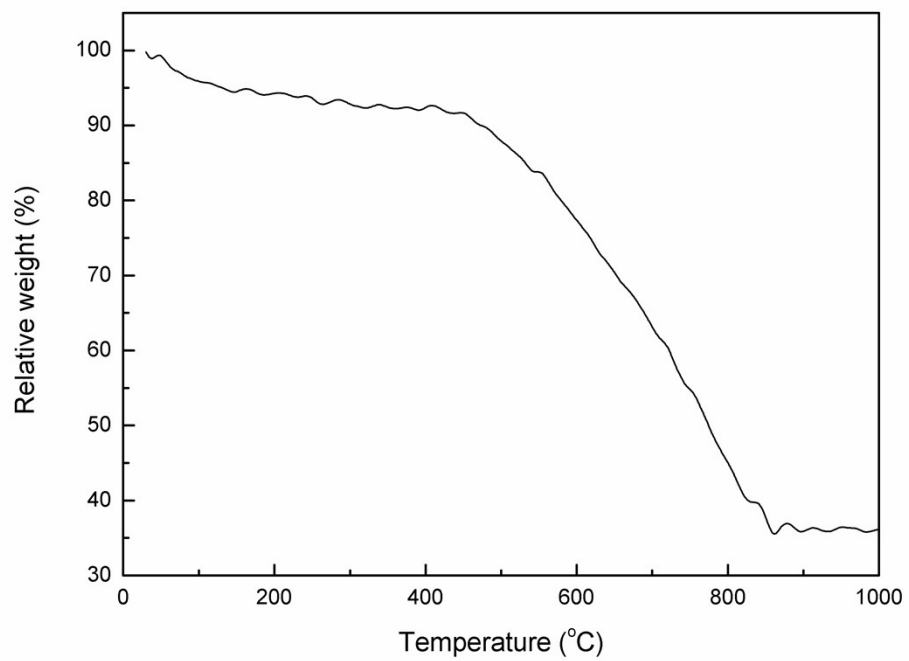


Fig. S3 Thermogravimetric analysis curves of Fe/OMC.

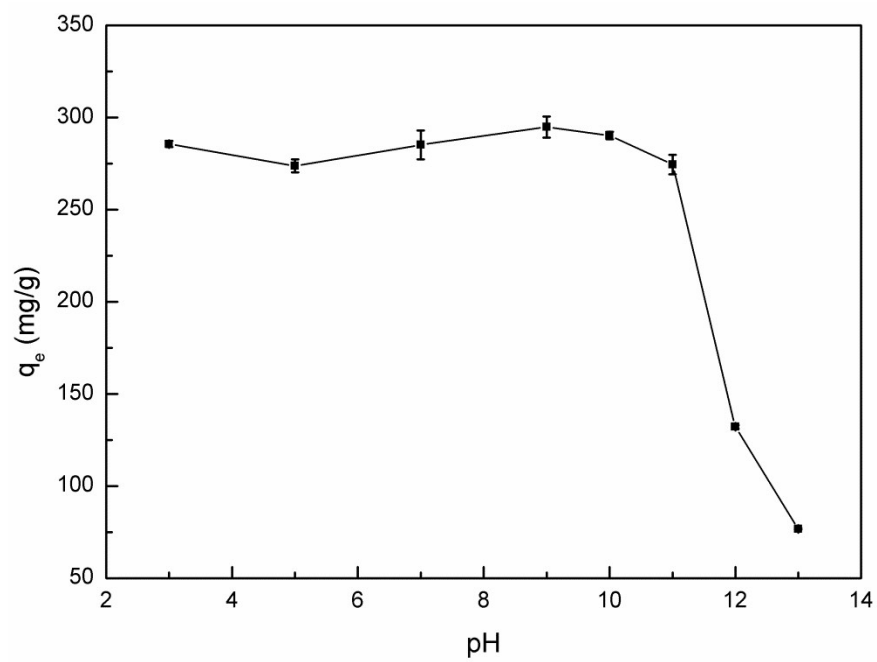


Fig. S4 Effect of pH values on removal of BPA by Fe/OMC at 25 °C, within 6h (initial concentration, 200 mg/L)

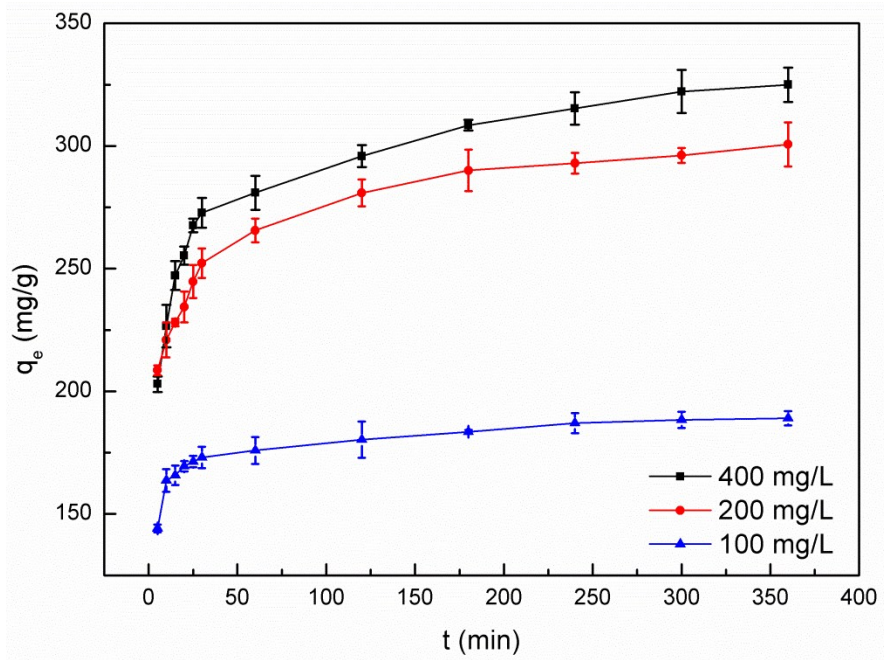


Fig. S5 Effect of contact time and initial concentration on removal of BPA by Fe/OMC at 25 °C

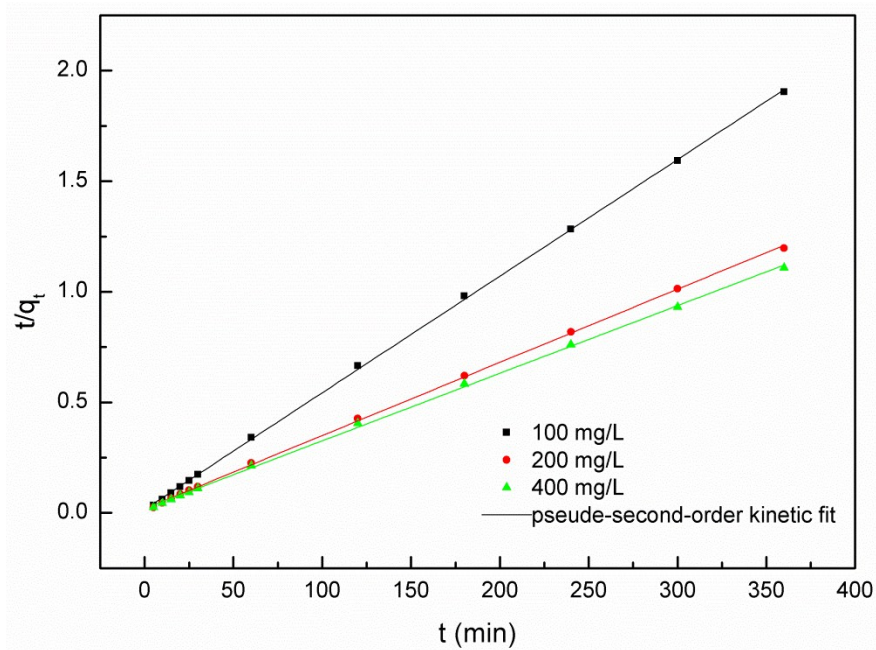


Fig. S6 Pseudo-second-order kinetic model for the adsorption of BPA onto Fe/OMC at 25 °C

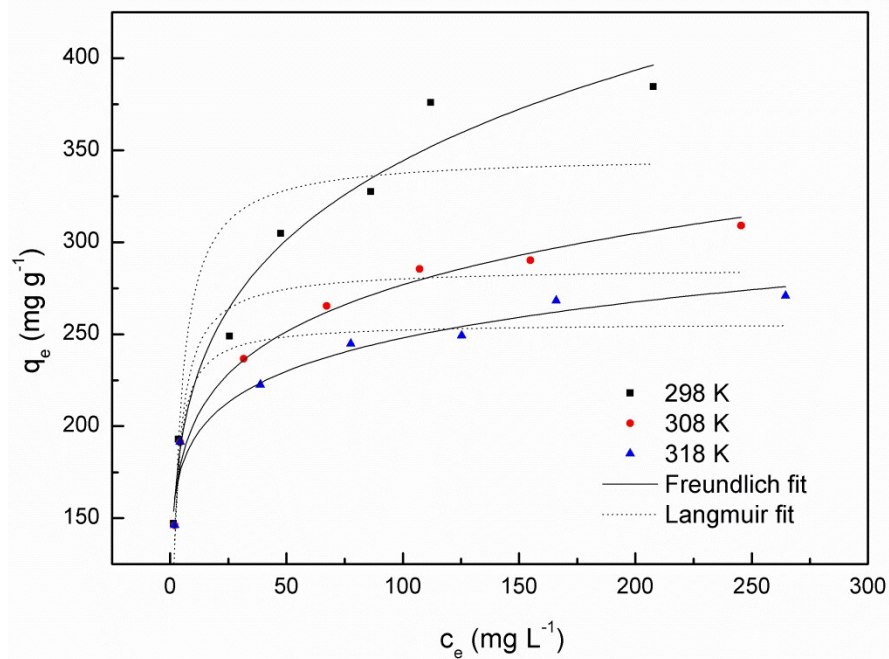


Fig. S7 Adsorption isotherms for adsorption of BPA onto Fe/OMC

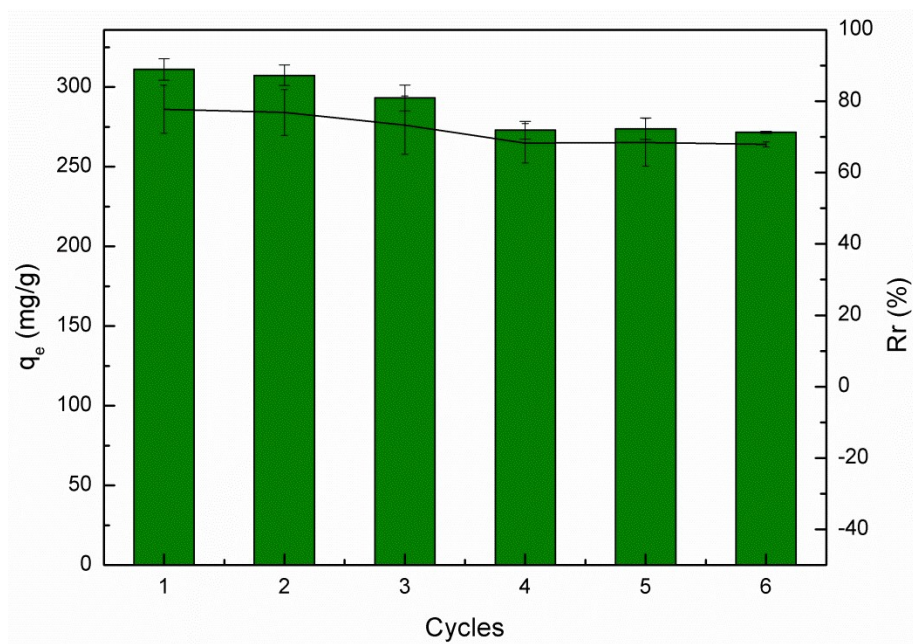


Fig. S8 Six consecutive adsorption–desorption cycles of Fe/OMC

Table S1

Pore structure parameters of the two mesoporous materials.

Samples	Surface area (m ² /g)	Pore size (nm)	Pore volume (cm ³ /g)
OMC	1620	4.9	2.3
Fe/OMC	536	3.8	1.1

Table S2

The chemical characterization results obtained by each analytical technique

Analytic technique	Observations
Scanning electron microscope/transmission electron microscopy	<ul style="list-style-type: none"> • Fe/OMC composite possessed uniform mesopores structure; • The degree of order was slightly lower than OMC ; • The iron nanoparticles with an average diameter about 20 nm were dispersed evenly on the carbon rod matrix
Nitrogen adsorption-desorption	The pore structure parameter values of Fe/OMC distinctly decreased compared with OMC, which might indicate that the iron nanoparticles changed the structure of carbon matrix or entered into channels partially occupying or even blocking the mesopores.
The Zeta potential	The zero point of zeta potential of Fe/OMC was at pH 4.76.
The vibrating sample magnetometer	The saturation magnetization strength of Fe/OMC was 10.54 emu/g which was beneficial for separation.
Thermogravimetric analysis	The weight percentage of Fe nanoparticles in Fe/OMC was 35.6 wt%.
Effect of initial pH	The removal capacity of Fe/OMC composite remained in high level (around 280 mg/g) at a wide pH range from 3 to 9.
Effect of contact time	<ul style="list-style-type: none"> • The removal process reached balance at about 6 h; • The experiment data exhibited good accordance with pseudo-second-order model.
Sorption isotherms	Freundlich isotherm model was more suitable for the adsorption of BPA by Fe/OMC than Langmuir model.
Thermodynamics	According to the thermodynamic parameters of enthalpy change ($\Delta H = -20.84$ KJ/mol), entropy change ($\Delta S = -56.74$ J/mol K) and free energy change ($\Delta G < 0$), the removal process of BPA by Fe/OMC was inferred to be thermodynamic feasible, unconscious, and spontaneous.
X-ray diffraction	Iron in Fe/OMC was mainly in the forms of nanoscale zero-valent iron and Fe ₃ O ₄ or Fe ₂ O ₃ .
Fourier transform infrared spectrometer	Most of the peaks of BPA-adsorbed Fe/OMC spectra were in accordance with the peaks from the FTIR spectrum of BPA indicated that a mass of BPA molecules were

X-ray photoelectron spectroscopy	adsorbed onto Fe/OMC. Detailed XPS spectrum of the regions for Fe 2p, O 1s and C 1s of the fresh and spent composites suggested the adsorption and degradation of BPA by Fe/OMC.
Regeneration of Fe/OMC	In the sixth absorption–desorption cycle, the removal efficiency as high as 68% was obtained, which suggested that Fe/OMC had a good performance for regeneration and reusability.
